Integrated Seismic Studies at the Rye Patch Geothermal Reservoir

R. Gritto, T. M. Daley and E. L. Majer
Lawrence Berkeley National Laboratory
1 Cyclotron Road
Berkeley, California 94720

Keywords: 3-D Surface Seismic Study, Rye Patch, Seismic-Wave-Fault-Interaction

Abstract

A 3-D surface seismic reflection survey, covering an area of over 3 square miles, was conducted at the Rye Patch geothermal reservoir (Nevada) to explore the structural features that may control geothermal production in the area. In addition to the surface sources and receivers, a high-temperature three-component seismometer was deployed in a borehole at a depth of 3900 ft within the basement below the reservoir, which recorded the waves generated by all surface sources. A total of 1959 first-arrival travel times were determined out of 2134 possible traces. Two-dimensional ray tracing was performed to simulate wave propagation from the surface sources to the receiver at depth. Travel time differences between observed and calculated times were mapped to topographic changes in the elevation of the interface between the carbonate basement and the sedimentary and volcanic unit above. Results indicate the presence of two dominant geologic features. The first confirms the regional trend of the geologic units in the Basin and Range province with a north-south strike and dip to the west, as expected for normal faulting encountered in an extensional regime. The second is a local disturbance of this regional pattern in form of an elevation of the interface between the carbonate basement and the overlying sedimentary sequence, striking east-west. The geometry of the structure is corroborated by results from a seismic-reflection survey, and by results of tomographic studies conducted as part of the seismic survey. Seismic waves, generated from far-offset shots during the 3-D surface survey, exhibit a sudden decrease in amplitudes while propagating across the boundaries of the elevation high. This apparent boundary correlates spatially with the location of the Rye Patch fault as interpreted from the 3-D seismic reflection data. Finite-difference modeling of elastic wave propagation is performed to estimate the structural parameters of the fault. Questions to be answered are fault width, strike, dip, and strength, to make inferences about the nature of the fault and the geologic process that could have formed it.

Introduction

In recent years, seismic surface and borehole experiments were conducted at the Rye Patch geothermal reservoir, Nevada, to determine the geologic structure of the (hypothesized) fault-controlled reservoir. The Rye Patch reservoir is located in Pershing County, Nevada, along the east side of Interstate 80, about 200 km northeast of Reno.

Commercial development of the Rye Patch geothermal project started in the late 1980s and resulted in the construction of a 12 MW powerplant and eight geothermal wells, of which seven were either too cold or had no fluid flow. In the successful well, however, significant production at reservoir temperatures in access of 200^{o}C were encountered. The eight boreholes were drilled within an area of less than one square mile, which indicated that distribution of reservoir fluids is most likely controlled by fractures and faulting with limited areal extent.

Lawrence Berkeley National Laboratory (LBNL) has cooperated with The Industrial Corporation (TIC) and Transpacific Geothermal Inc. (TGI) in studies to evaluate and apply modern seismic imaging methods for geothermal reservoir definition under the U.S. Department of Energy's (DOE) Geothermal Program. As part of this cooperation a vertical seismic profile (VSP) was acquired in 1997, at the Rye Patch geothermal field in Nevada, to determine the structure of the reservoir. The VSP survey was conducted to determine the seismic reflectivity of the reservoir horizons and to obtain reservoir velocity information. Because the results of the initial VSP indicated apparent reflections at depth (Feighner et al., 1998), it was decided to proceed with a 3-D seismic surface survey which was completed in 1998.

As part of the seismic surface survey, an additional surface-to-borehole experiment was conducted, during which a three-component high-temperature geophone was installed in the original VSP well at a depth of 3900 ft. This geophone recorded all seismic waves generated by the surface sources, creating a second data set in addition to the seismic-reflection data. The locations of the 3-D surface survey and of borehole 46-28 containing the geophone at depth are indicated in Figure 1 (modified after GeothermEx). The survey overlaps the Rye Patch temperature anomaly, which is bounded by the Humbold City Thrust in the East and the Rye Patch reservoir in the West. Results of the 3-D seismic survey were presented by Feighner et al. (1999) and revealed possible faulting at depth based on surface seismic-reflection studies and surface-to-surface tomographic-travel-time investigations.

In the current study, we present a synthesis of the results of the seismic surveys and derive a structural fault model that could explain the interesting wave propagation effects that are present in the seismic data sets.

Data Acquisition and Quality

The Rye Patch seismic surface survey covered an area of over 3 square miles and had 12 north-south receiver lines and 25 east-west source lines. The source interval was 100 feet while the source line spacing was 400 feet. Four Litton 311 vibrators were used in a square array with the source point at the center of the array. The source signal was a sweep with a frequency bandwidth between 8 Hz and 60 Hz. Figure 2 shows a layout of the survey area. The surface survey recorded over one million seismic traces.

In addition to the surface survey, a high temperature, wall-locking, three-component geophone was installed in well 46-28 at 3900 ft depth. The borehole geophone recorded all shots throughout the survey area, creating a second data set with a total of 2134 traces. The data quality of the borehole data is good with a frequency content of about 25 Hz for the first arriving waves. This second data set is used to model seismic wave propagation from the surface and the geophone at depth, and to map differences between synthetic and field data into topography changes

Seismic Mapping of Subsurface Topography

Mapping travel-time deviations to elevation changes is a technique that has been used in seismic refraction studies in the past (Dix, 1952). The method is an approximation that can be applied to environments where a low-velocity layer is located above a high-velocity layer. Under the assumption that the ray path from source to receiver is known, any difference between the calculated and observed travel times is converted into a distance using the velocity model and applied as a deviation in the boundary between the two layers. The same principle is applied in the current approach assuming that the top layer is represented by the sedimentary and volcanic Tertiary sequence, whereas the Triassic carbonates of the basement are represented by a halfspace.

The P-wave velocity profile derived from the 1997 VSP experiment, represents the best estimate for the distribution of velocities in the subsurface around the well, and is the only *in situ* velocity measurement available. This velocity profile was extended to a 2-D velocity model throughout the survey area. Based on this model, 2-D ray tracing is performed to simulate wave propagation from surface sources to the borehole geophone at depth. Figure 3 shows the results of the ray tracing for two representative source lines. Figure 3a represents the rays for a source line that runs in an east-west direction across well 46-28, while Figure 3b shows a line running across the well in a north-south direction. The gaps in source coverage indicate the railroad tracks, Interstate 80, and an area in the vicinity of the well where no sources were fired. The calculated times are compared to the observed times and differences are converted to elevation changes in the boundary between the basement and the overlying layer.

Results of Seismic Studies

Figure 4 shows a contour plot of the results of the seismic mapping. The contour lines represent the topography of the basement interface. The three boreholes 46-28, 44-28, and 42-28 are shown for reference. It can be seen that the 0 m elevation contour line runs through well 46-28, which is a confirmation that the velocity model shown in Figure 3 is a good representation of the actual velocities in the vicinity of the VSP well 46-28. The map indicates the presence of two structural features. In the western half of the survey area a pronounced trend to negative elevation changes could indicate a rapid deepening

of the basement to the west created by north-south trending normal faults, which constitute the dominant structural mechanism in the Basin and Range province. The second feature is an elevation high that extends from east to west, and elevates the basement interface in the east while cutting through the steep descent on the western flank.

In addition to the source locations shown in Figure 2, four far-offset source locations were selected during the 3-D seismic survey in 1998, to obtain far-offset refracted first-arrival data that could be used to determine the deeper velocity structure. The far offset shots were recorded by 10 receiver lines in the center of the survey. Data quality varied significantly for each of the four shots, indicating regional heterogeneity. The qualitatively best data sets resulted from shot number 2, located 4.6 miles NW of the VSP well 46-28, and shot number 4, located 3.2 miles SSE of the well.

Figure 5 shows the data for far-offset shot number 2 recorded by a receiver line in the western half of the survey area. The northern receivers recorded sharp first arrivals, but the signal is abruptly attenuated for the receivers in the central and southern part of the survey area. This pattern was consistent for the other receiver lines. The two gray areas in Figure 11 represent the receiver locations where the first-arrival energy was clearly visible. The northern polygon represents the arrivals of the data recorded from shot number 2 to the northwest, while the southern polygon represents those of shot number 4 to the south. It is evident from the figure that the central area had weak or non-existing first arrival energy. A possible interpretation is the existence of faults where seismic energy is scattered and attenuated. Since the boundaries of the polygons match the outline of the elevated structure quite well, it could be concluded that faults, bounding the elevated structure to the north and south, attenuated the seismic waves from the far offset shots.

The location of a possible fault was interpreted by Teplow (1999) based on 3-D seismic reflection data. The intersection of the fault with the clastic reservoir unit had a strike of N76^{o}W and a dip of 73^{o}NNE. The intersection of this fault with the sedimentary-carbonate interface is indicated by the dark-gray line in Figure 4, immediately south of well 44-28. The interpretation of the east-west extension of the fault was limited because of the poor continuity of reflected seismic energy in the east-west direction. It can be seen that the strike-line of the fault coincides with the boundary of the southern zone that marks the transition from strong to weak first arrival energy, and is co-located with the southern flank of the elevated structure indicated by the contour lines. Thus a possible interpretation is that the elevated structure is a manifestation of the postulated fault.

The spectral content of the elastic waves shown in Figure 5 contains information about the medium that the waves propagated through. Figure 6 redisplays the receiver gather shown in Figure 5 in conjunction with the spectral information of the data. It is evident that most of the spectral energy in the frequency band between 15 and 30 Hz is attenuated cross the receiver array. This attenuation mechanism will be investigated using elastic waveform modeling, based on the geometry of the surface seismic survey. Numerically generated data will be compared to field data. The results will provide estimates of fault

width, strike, dip, and possible strength of the fault zone (i.e., whether the fault core consists of soft gauge or densified hydrothermally-altered material).

Conclusions

The geophysical experiments conducted at Rye Patch geothermal field provided various data sets that helped to interpret the subsurface structure of the reservoir. The addition of a depth geophone to record surface generated seismic waves during the 3-D reflection survey provided an additional independent data set at low cost and with minimum technical and labor requirements. Because most geothermal areas provide access to open boreholes during the developing stages of the reservoir, it is recommended that a VSP survey is conducted first, to obtain information about the velocity structure and the reflectivity of the subsurface. These in situ measurements are the only direct methods to determine seismic velocities at depth, and are imperative for the planing of any future surface seismic reflection surveys.

The current study would have benefited from additional VSP data, which could have generated a more realistic velocity model. If it is determined that a surface seismic-reflection survey may provide more detailed information about the reservoir structure, we recommend adding geophones to any available borehole within the survey area. These data sets collected at depth provide an independent, low-cost alternative to the surface data and can help in the interpretation of the subsurface structure.

Seismic mapping is a robust method for converting travel-time differences to elevation changes, but it is an approximation that relies on a predefined reference velocity model. The results confirm the regional structure of the Basin and Range province. The general trend of the geologic units reveal a north-south strike and dip to the west, as expected for normal faulting encountered in the extensional regime of the Basin and Range province. Furthermore, a local disturbance of this general pattern is detected by an elevation of the interface between the carbonate basement and the overlying sedimentary sequence. The structure, which resembles a horst, strikes east-west and appears to be extending throughout the survey area, cross-cutting the westward dipping units along the western boundary of the survey area. Previous studies corroborate the findings of the current work, because the boundaries of the elevated structure co-locate with areas in which the first arrivals of seismic waves undergo a transition from strong to weak amplitudes. The spectral losses of the seismic waves propagating through fault systems can be used to determine fault-structural parameters.

Acknowledgments

This work was supported by the Assistant Secretary for Energy Efficiency and Renewable Energy, Office of Wind and Geothermal Technologies, of the US Department

of Energy under Contract No. DE-AC03-76SF00098. Data processing was performed at the Center for Computational Seismology, which is supported by the Director, Office of Science, Office of Basic Energy Sciences, Division of Engineering and Geosciences, of the U.S. Department of Energy under Contract No. DE-AC03-76SF00098.

References

Dix, C. H., 1952, Seismic prospecting for oil, Harper, New York, pp. 414.

Feighner, M.A., Daley, T.M., Majer, E.L., 1998. Results of the Vertical Seismic Profiling at Well 46-28, Rye Patch Geothermal Field, Pershing County, Nevada, Lawrence Berkeley National Laboratory Report LBNL-41800.

Feighner, M., Gritto, R., Daley, T.M., Keers, H., Majer, E.L., 1999, Three-Dimensional Seismic Imaging of the Rye Patch Geothermal Reservoir, Lawrence Berkeley National Laboratory Report LBNL-44119.

Teplow, B., 1999. Integrated Geophysical Exploration Program at the Rye Patch Geothermal Field, Pershing County, Nevada, Final Report to Mount Wheeler Power.

Figure Captions

Figure 1: Rye Patch Geothermal Field. Location map showing 3-D survey area and VSP Well 46-28.

Figure 2: Source and receiver geometry of seismic survey. Sources are indicated by stars, while receivers are indicated by small circles. Boreholes are indicated by big circles.

Figure 3: Velocity model and ray paths from source lines transecting well 46-28:
(a) N-S direction; (b)E-W direction.

Figure 4: Contour map of the variations in elevation of the basement interface. The gray areas represent receiver locations where good first-arrival energy was recorded from far-offset shots during the 3-D seismic survey. The northern area recorded good first-arrival energy from shot number 2, located to the NW of the VSP well 46-28, while the southern area recorded good first arrival energy from shot number 4, located SSE of the VSP well. The bold gray line represents the projection of a fault onto the basement interface that was interpreted by Teplow (1999) from 3-D seismic reflection data.

Figure 5: Seismic data recorded along a representative receiver line in the western part of the survey area. The source position was at shot number 2. Notice the abrupt change in amplitudes of the first arrivals, as indicated by the arrow.

Figure 6: (a) Common source gather of shot number 2 and (b) frequency spectrum as a function of offset. The gap in spectral energy beyond trace number 34 is caused by attenuation of the elastic waves during propagation across the fault.

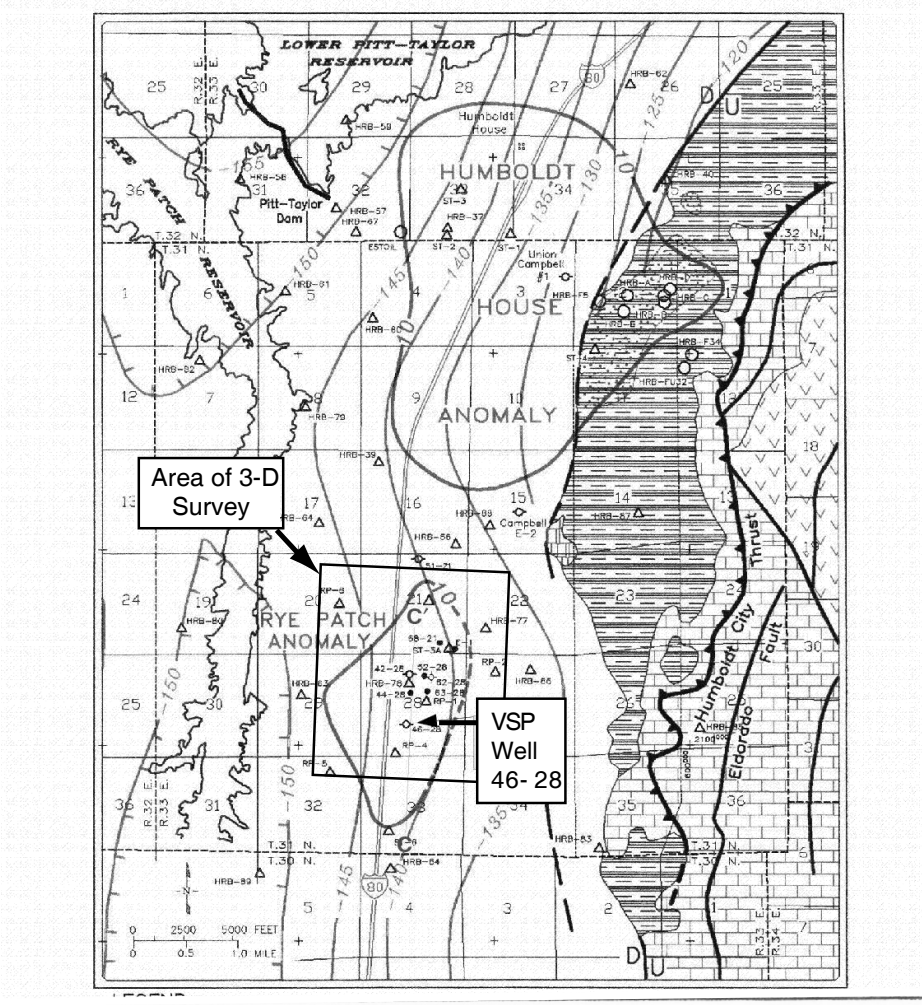

-140- Line of equal complete bouguer gravity. Assumes a bedrock density of 2.67 g/cm^3 (interval 5 mgals)

—10— Shallow temperature gradient contour, °F/100'

● / ○ Capable of production / dry hole

△ / ○ Strat test or gradient hole / mineral test hole

✧ Plugged & abandoned well

U / D Normal fault (dashed where inferred)

Thrust fault (teeth on upper plate)

Hydrothermally altered area

Quaternary alluvium or lake deposits

Tertiary basalt

Triassic Grass Valley Fm. (metamorphosed mudstone and sandstone)

Triassic Star Peak Group limestone (Natchez Pass and Prida Formations)

Triassic rhyolite porphyry and ash-flow tuff

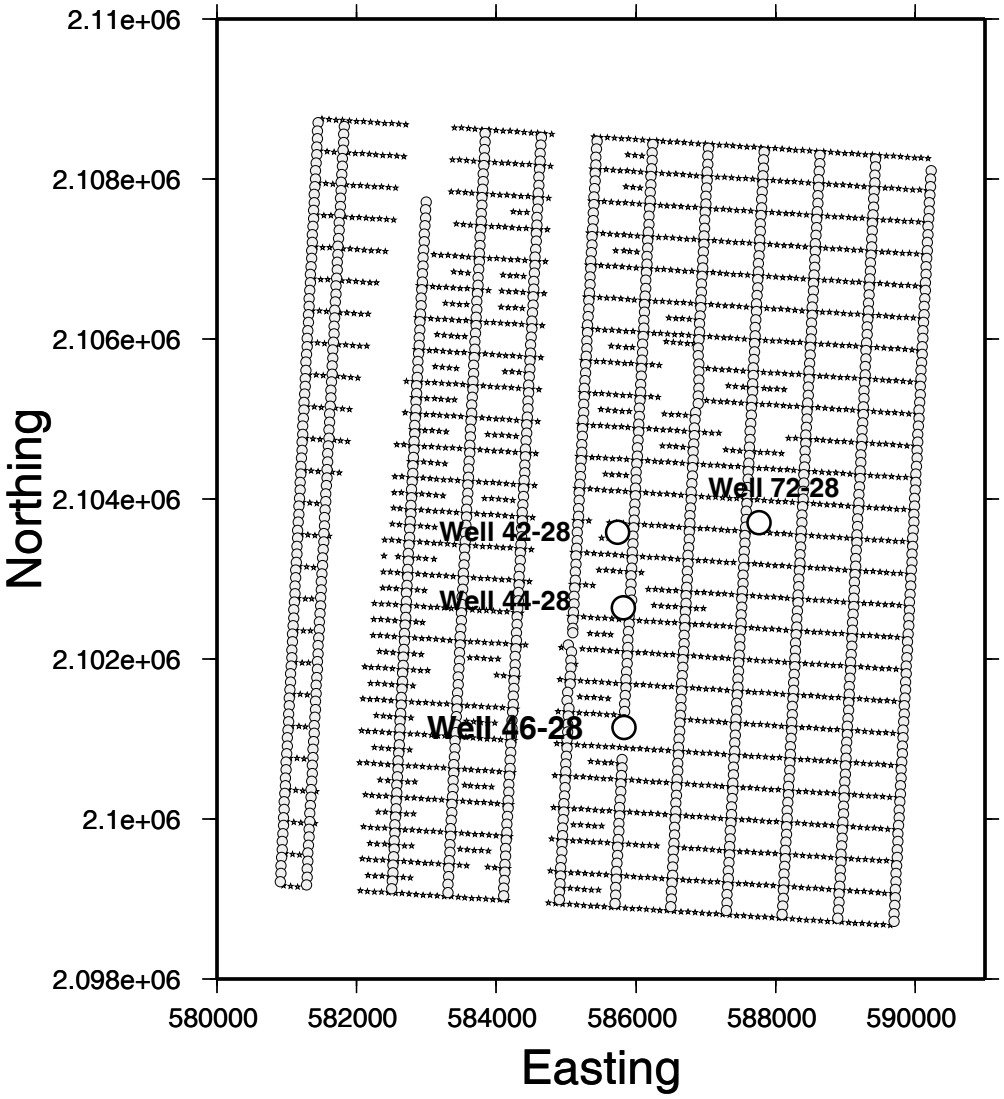
2.11e+06
2.108e+06
2.106e+06
2.104e+06
2.102e+06
2.1e+06
2.098e+06
Northing
580000
582000
584000
586000
588000
590000
Easting
Well 72-28
Well 42-28
Well 44-28
Well 46-28

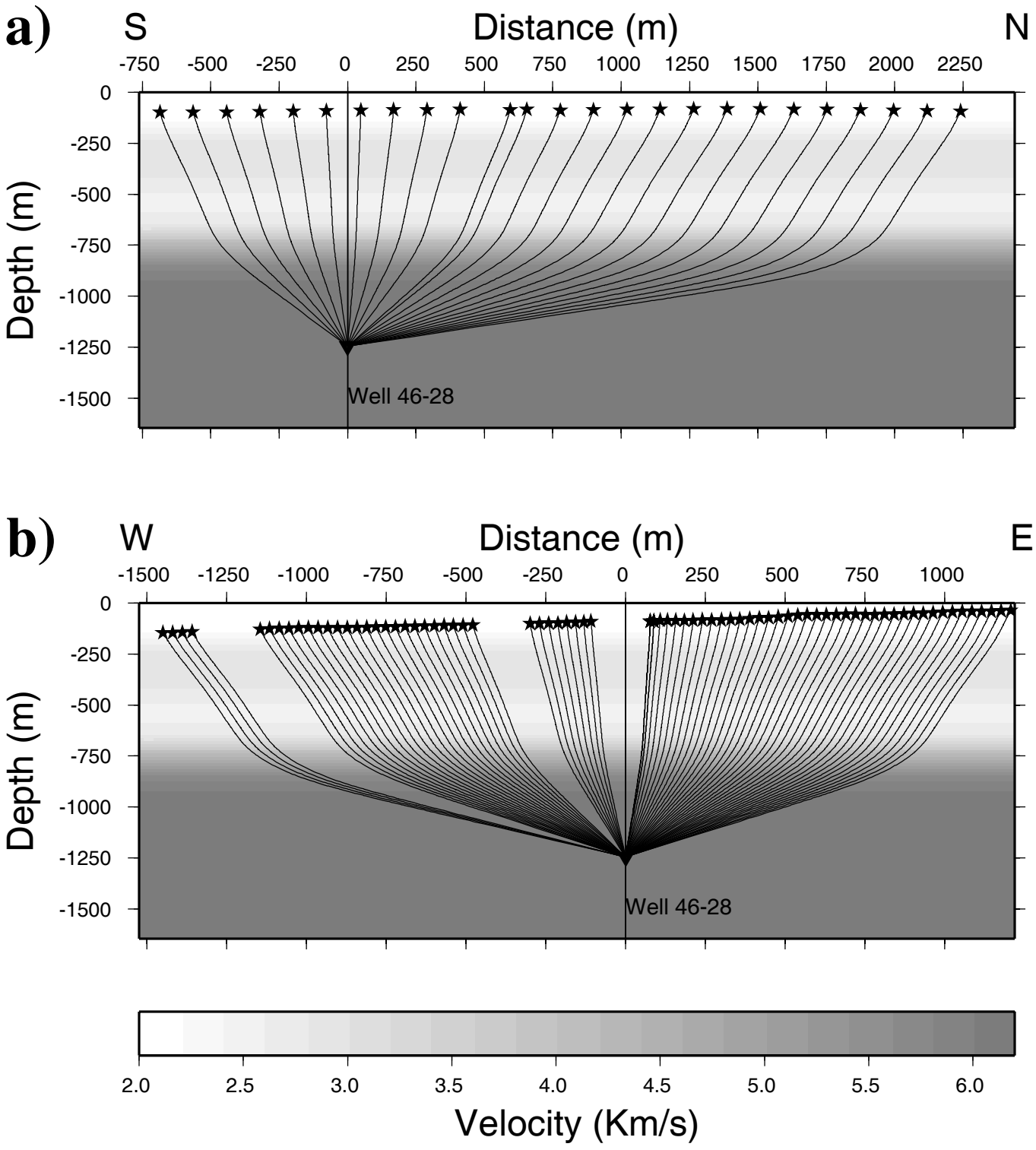
a)
S
Distance (m)
N
-750 -500 -250 0 250 500 750 1000 1250 1500 1750 2000 2250
0
-250
-500
-750
-1000
-1250
-1500
Depth (m)
Well 46-28
b)
W
Distance (m)
E
-1500 -1250 -1000 -750 -500 -250 0 250 500 750 1000
0
-250
-500
-750
-1000
-1250
-1500
Depth (m)
Well 46-28
2.0 2.5 3.0 3.5 4.0 4.5 5.0 5.5 6.0
Velocity (Km/s)

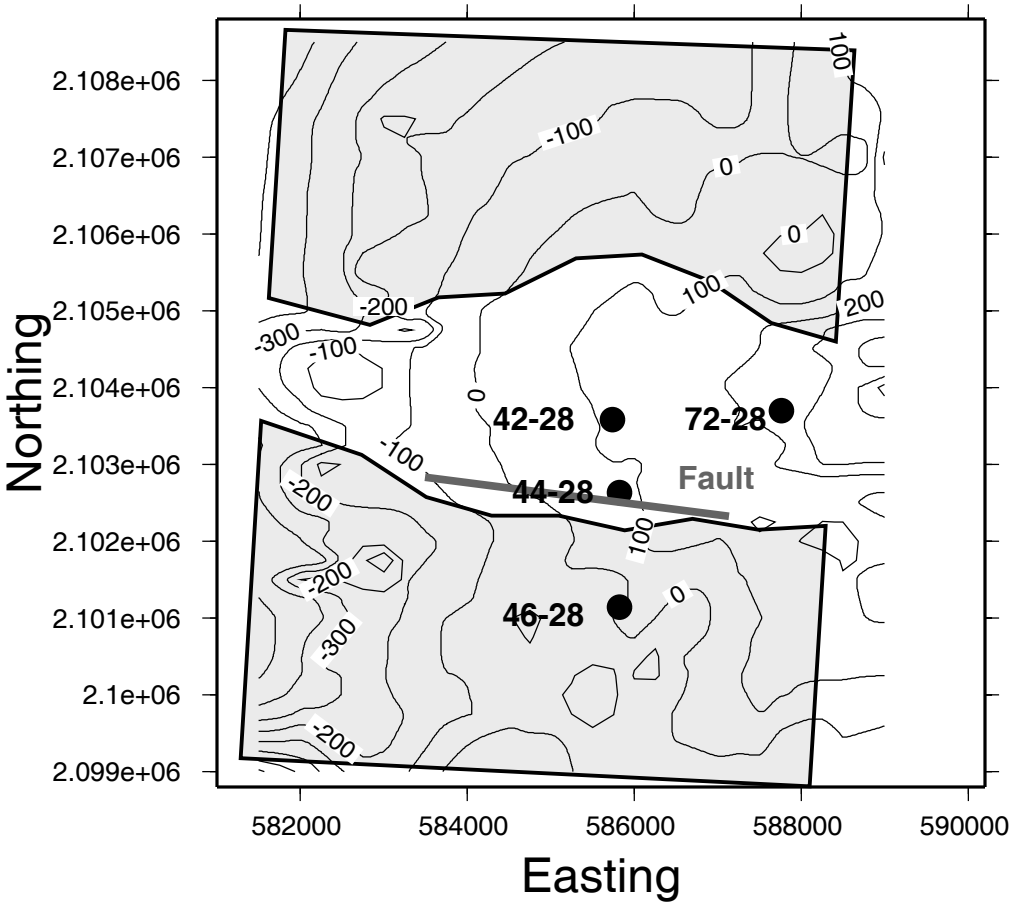
Northing
Easting
2.108e+06
2.107e+06
2.106e+06
2.105e+06
2.104e+06
2.103e+06
2.102e+06
2.101e+06
2.1e+06
2.099e+06
582000
584000
586000
588000
590000
100
-100
0
0
-200
100
200
-300
-100
0
42-28
72-28
-100
Fault
44-28
-200
100
-200
46-28
0
-300
-200

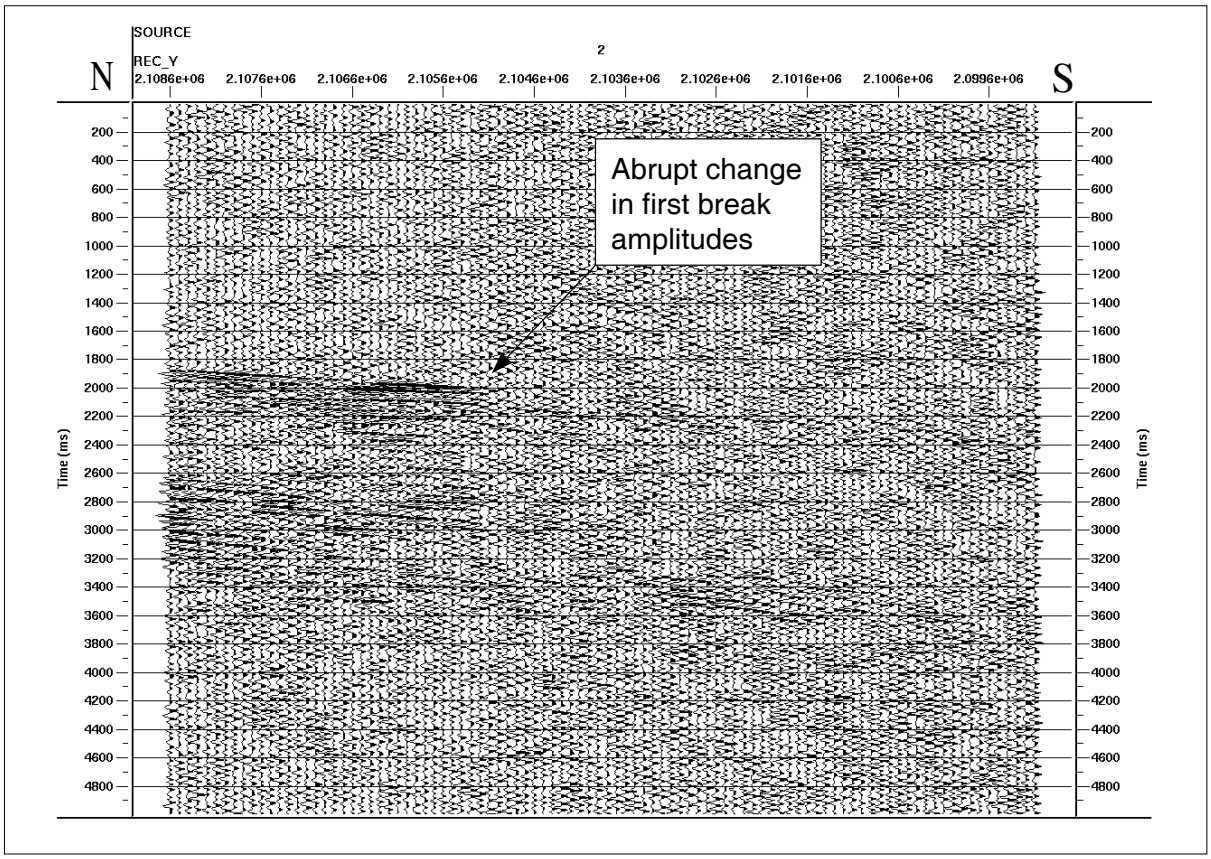
SOURCE
2
N
REC_Y
2.1086e+06
2.1076e+06
2.1066e+06
2.1056e+06
2.1046e+06
2.1036e+06
2.1026e+06
2.1016e+06
2.1006e+06
2.0996e+06
S
Abrupt change in first break amplitudes
Time (ms)
200
400
600
800
1000
1200
1400
1600
1800
2000
2200
2400
2600
2800
3000
3200
3400
3600
3800
4000
4200
4400
4600
4800

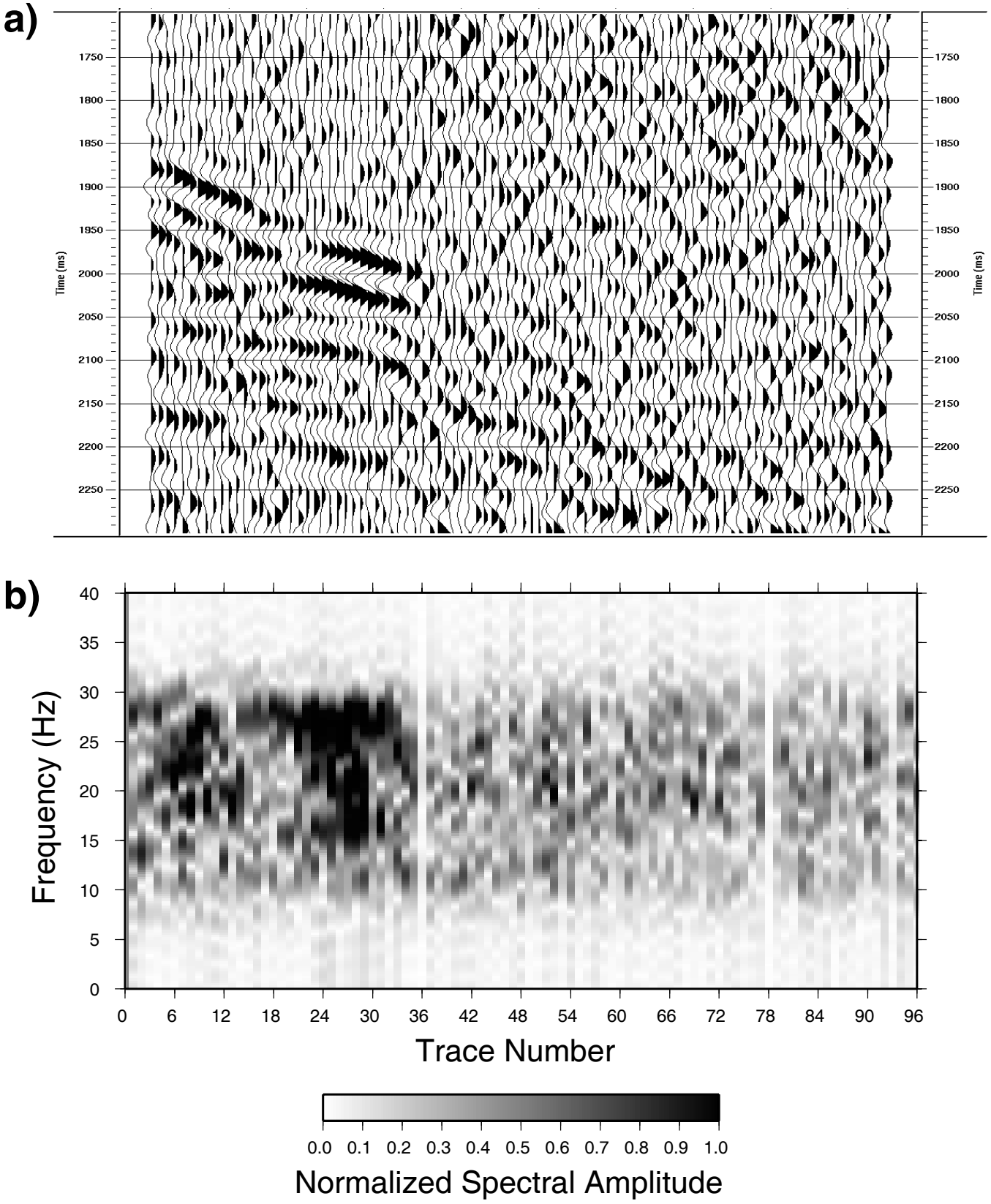
a)
Time (ms)
1750
1800
1850
1900
1950
2000
2050
2100
2150
2200
2250
b)
Frequency (Hz)
0
5
10
15
20
25
30
35
40
0
6
12
18
24
30
36
42
48
54
60
66
72
78
84
90
96
Trace Number
0.0
0.1
0.2
0.3
0.4
0.5
0.6
0.7
0.8
0.9
1.0
Normalized Spectral Amplitude